Formation of a standing-light pulse through collision of gap solitons

William C. K. Mak,[1] Boris A. Malomed,[2,1] and Pak L. Chu[1]
[1]*Optoelectronic Research Centre, Department of Electronic Engineering, City University of Hong Kong, Hong Kong*
[2]*Department of Interdisciplinary Studies, Faculty of Engineering, Tel Aviv University, Tel Aviv 69978, Israel*
(Received 31 October 2002; revised manuscript received 30 April 2003; published 22 August 2003)

Results of a systematic theoretical study of collisions between moving solitons in a fiber grating are presented. Various outcomes of the collision are identified, the most interesting one being merger of the solitons into a single zero-velocity pulse, which suggests a way to create pulses of ''standing light.'' The merger occurs with the solitons whose energy takes values between 0.15 and 0.35 of the limit value, while their velocity is limited by ≈ 0.2 of the limit light velocity in the fiber. If the energy is larger, another noteworthy outcome is acceleration of the solitons as a result of the collision. In the case of mutual passage of the solitons, inelasticity of the collision is quantified by the energy-loss share. Past the soliton's stability limit, the collision results in strong deformation and subsequent destruction of the solitons. Simulations of multiple collisions of two solitons in a fiber-loop configuration are performed too. In this case, the maximum velocity admitting the merger increases to ≈ 0.4 of the limit velocity. The influence of an attractive local defect on the collision is also studied, with the conclusion that the defect does not alter the overall picture, although it traps a small-amplitude pulse. Related effects in single-soliton dynamics are considered too, the most important one being the possibility of slowing down the soliton (reducing its velocity to the above-mentioned values that admit fusion of colliding solitons) by passing it through an apodized fiber grating, i.e., one with a gradually increasing Bragg reflectivity. Additionally, transformation of an input sech signal into a gap soliton (which is quantified by the share of lost energy), and the rate of decay of a quiescent gap soliton in a finite fiber grating, due to energy leakage through loose edges, are also studied.

DOI: 10.1103/PhysRevE.68.026609 PACS number(s): 42.81.Dp, 42.50.Md, 42.65.Tg, 05.45.Yv

I. INTRODUCTION

Bragg gratings (BGs) are structures in the form of a periodic variation of the core refractive index, which are written on a fiber or other optical waveguide [1]. Devices based on fiber gratings, such as filters and gain equalizers, are among the most widely used components of optical systems. *Gap solitons* (in a more general context, they are called BG solitons [2]) exist in fiber gratings due to the interplay between the BG-induced effective dispersion (which includes a gap in the system's linear spectrum) and the Kerr nonlinearity of the fiber's core. Exact analytical solutions for BG solitons in a fiber-grating model were found in Refs. [3,4], and their stability was studied later, showing that approximately half of them are stable (see details below) [5,6]. Spatial solitons and their stability in a model of a planar BG-equipped waveguide, taking into regard two polarizations of light, were recently considered in Ref. [7].

Lately, a lot of attention has been attracted to the possibility of capturing ''slow light'' [8], and, in particular, of slowly moving optical solitons [9] in various settings. The fiber grating is a natural candidate for a nonlinear medium where it may be possible to stop the light, as exact solutions for zero-velocity BG solitons, in which the left- and right-traveling waves are in permanent dynamical equilibrium, are available in the corresponding model [3,4], and some of them are stable [5,6]. However, BG solitons that were observed in the first experiments were fast ones, moving at a velocity $\approx 75\%$ of the limit light velocity in the fiber [10]. A possible way to capture a zero-velocity soliton is to use an attractive finite-size [11] or δ-like [12] local defect in the BG which attracts solitons (it was demonstrated in Ref. [13] that a defect can also stimulate a nonlinear four-wave interaction without formation of a soliton). Moreover, it is possible to combine the attractive defect with local gain, which opens a way to create a permanently existing pinned soliton, even in the presence of loss [14].

One of the objectives of this paper is to explore the possibility of creating standing BG solitons as a result of a head-on collision between two identical moving ones. Collisions are quite feasible from the experimental standpoint, as the characteristic length necessary for the formation of a BG soliton is $\simeq 2$ cm [10], while uniform fiber gratings with a length of 1 m or even longer are now available. In [3], where exact solutions for the moving solitons were found, their collisions were already simulated, with the conclusion that they passed through each other developing intrinsic vibrations, which may be explained by excitation of an intrinsic mode which a stable BG soliton supports [5].

Actually, broad small-amplitude BG solitons are asymptotically equivalent to nonlinear-Schrödinger (NLS) solitons, and hence collisions between them are completely elastic [15]. However, in a more generic case results may be different, as the standard fiber-grating model [see Eqs. (1) below] is not an integrable one, in contrast to the NLS equation. Systematic simulations are thus needed to study head-on collisions between BG solitons, the results of which are reported below (in Sec. IV, after presenting the model in Sec. II, and considering the one-soliton solution in Sec. III). The main finding is that, at relatively small values of the soliton velocity $\pm c$, and not too large values of the soliton energy, in-phase solitons merge into a single *standing* one. We find the maximum velocity c admitting the merger, which is ≈ 0.2 of the maximum light velocity in the fiber.

As mentioned above, in the first experiments the BG solitons were observed with the velocity ≈ 0.75; hence it is necessary to slow down the solitons before the collision, bridging the gap between the velocity values 0.75 and 0.2, if the formation of a standing pulse is an objective. Using the well-known technique based on the balance equation for the soliton's momentum [16], we demonstrate in Sec. III that the slowing down can be achieved in a so-called apodized grating, i.e., one with the grating strength (Bragg reflectivity) subject to a slow variation along the fiber. In fact, apodized gratings are easily fabricated and commonly used for other applications (in particular, to facilitate coupling of light into the grating) [1]. We demonstrate that reducing the soliton's velocity from 0.75 to 0.2 requires enhancing the Bragg reflectivity by a rather modest factor ≈ 1.48.

In the case when the solitons pass through each other, we quantify the collision by the energy-loss share. Sec. IV includes diagrams which display, in the plane of the soliton's velocity and energy, all possible outcomes of the collision between both in-phase and π-out-of-phase solitons. In the former case, possible outcomes are, in addition to the merger, passage of the solitons with decrease or *increase* of their velocities, and destruction of the solitons in the case when their energy is too large.

In Sec. V, we report the results of simulations of multiple collisions between two solitons, to model the situation in a fiber loop. Although experiments with a loop composed solely of a fiber grating have not yet been reported, numerous experiments have been done for various fiber-ring setups that include a passive or active pump and one or several BGs as a crucially important ingredient [17–19]. In particular, stable circulation of picosecond temporal pulses was observed in ring resonators of this type [19]. We demonstrate that multiple collisions between BGs in the loop are important in increasing the maximum velocity that admits the merger from the above-mentioned value ≈ 0.2 to ≈ 0.4 of the maximum light velocity in the fiber.

We have also carried out simulations to check if inclusion of a local attractive defect may assist the fusion of colliding solitons. In Sec. VI, we demonstrate that the defect does not essentially affect the situation; however, a trapped pulse, which captures a small share of the initial energy of the solitons, appears as a result of the collision.

Finally, in Sec. VII we report some related results pertaining to single-soliton dynamics, viz., reshaping of an input pulse of a sech (NLS soliton) or Gaussian form into a BG soliton in the fiber grating, and gradual decay of a gap soliton in a finite-length grating due to the energy leakage through the open ends. Section VIII concludes the paper.

II. THE MODEL

The commonly adopted model of nonlinear fiber gratings is based on a system of coupled equations for the right- (u) and left- (v) traveling waves [2],

$$iu_t + iu_x + \kappa v + [(1/2)|u|^2 + |v|^2]u = 0,$$

$$iv_t - iv_x + \kappa u + [(1/2)|v|^2 + |u|^2]v = 0, \qquad (1)$$

where x and t are the coordinate and time, which are scaled so that the linear group velocity of light is 1, and κ is the Bragg-reflectivity coefficient. In the case of the uniform grating, Eqs. (1) can be additionally normalized so as to set $\kappa = 1$, which we do below. However, in the case of the apodized grating, κ is a function of x.

Exact solutions to Eqs. (1) with $\kappa \equiv 1$, which describe solitons moving at a velocity c ($c^2 < 1$), were found in Refs. [3] and [4]:

$$u = \alpha W(X) \exp[y/2 + i\phi(X) - iT\cos\theta + i\phi_0],$$

$$v = -\alpha W^*(X) \exp[-y/2 + i\phi(X) - iT\cos\theta + i\phi_0]. \quad (2)$$

Here, the asterisk stands for complex conjugation, and θ is an intrinsic parameter of the soliton family which takes values $0 < \theta < \pi$ and is proportional to the soliton's energy (alias the norm)

$$E \equiv \int_{-\infty}^{+\infty} [|u(x)|^2 + |v(x)|^2]dx = \frac{8\theta}{(3 + 2c^2)}. \qquad (3)$$

Further, $\alpha^{-2} \equiv \frac{3}{2} + c^2$, $\tanh y \equiv c$, ϕ_0 is an arbitrary real constant, and

$$X = (1 - c^2)^{-1/2}(x - ct), \quad T = (1 - c^2)^{-1/2}(t - cx),$$

$$\phi(X) = \alpha^2 \sinh(2y) \tan^{-1}\{\tanh[(\sin\theta)X] \tan(\theta/2)\}, \quad (4)$$

$$W(X) = (\sin\theta)\,\mathrm{sech}[(\sin\theta)X - i(\theta/2)].$$

Below, we use these exact solutions as initial conditions to simulate collisions between identical solitons with opposite velocities.

Lastly, to consider the influence of a local defect on the collision (see Sec. VI below), Eqs. (1) are modified as in Refs. [11] and [12]:

$$iu_t + iu_x + v + [(1/2)|u|^2 + |v|^2]u = -\delta(x)(\Gamma u - \kappa v), \qquad (5)$$

$$iv_t - iv_x + u + [(1/2)|v|^2 + |u|^2]v = -\delta(x)(\Gamma v - \kappa u), \qquad (6)$$

where $\Gamma > 0$ and $\kappa > 0$ account for a local increase of the refractive index and suppression of the Bragg reflectivity, respectively. In this case, we set $\kappa \equiv 1$ away from the point $x = 0$, cf. Eqs. (1).

III. SLOWING DOWN A SOLITON IN THE APODIZED FIBER GRATING

Before proceeding to the consideration of collisions proper, we analyze the possibility of controlling the velocity of a soliton in a BG where the reflectivity κ is subject to smooth variation along the fiber, which is described by Eqs. (1) with $\kappa = \kappa(x)$. To this end, we notice that the uniform BG with $\kappa = \text{const}$ conserves the field momentum,

$$P = \int_{-\infty}^{+\infty} (u_x^* u + v_x^* v)dx. \qquad (7)$$

The calculation of the expression (7) for the exact soliton solution given by the expressions (2) and (4), where κ is kept as a free constant parameter, rather than being set equal to 1, yields the soliton's momentum,

$$P_{\rm sol}=\frac{8\kappa c}{(3+2c^2)\sqrt{1-c^2}}\left[\theta\cos\theta+\frac{4(\theta+\sin\theta)\sin^2(\theta/2)}{(3+2c^2)(1-c^2)}\right] \tag{8}$$

(note that for small c the proportionality coefficient between P and c, i.e., the soliton's mass, is always positive).

If the reflectivity is subject to a spatial modulation $\kappa=\kappa(x)$, the momentum is not conserved; instead, it evolves in time according to the following equation, which directly follows from Eqs. (1):

$$\frac{dP}{dt}=2\int_{-\infty}^{+\infty}\frac{d\kappa}{dx}{\rm Re}(uv^*)dx. \tag{9}$$

In the case when a soliton with a velocity c moves in the apodized BG with slowly varying $\kappa(x)$, so that κ is almost constant on a spatial scale corresponding to the soliton's size, the gradient $d\kappa/dx$ can be written before the integral in Eq. (9), and then the remaining integral can be explicitly calculated in the first approximation, substituting the expressions (2) and (4) for the unperturbed soliton:

$$\frac{d}{dt}P_{\rm sol}=-\frac{8\sqrt{1-c^2}}{3+2c^2}\frac{d\kappa}{dx}[2(\sin\theta)(1+\cos\theta) -\theta(\cos\theta)(1+2\cos\theta)]. \tag{10}$$

The expression in the square brackets in Eq. (10) is always positive for $\theta\leq\pi/2$ (i.e., for stable solitons, see below), but it changes sign and becomes negative at $\theta>\theta_0\approx 0.73\pi$.

An effective equation for the velocity of the soliton in the apodized BG with smoothly varying $\kappa(x)$ can be obtained by substitution of the expression (8) into the left-hand side of Eq. (10) and taking into consideration that the soliton's energy, given by Eq. (3) (which is not altered if $\kappa\neq 1$) remains a dynamical invariant in the case of the x-dependent κ. In particular, in the case when $c^2\lesssim 1/2$, which corresponds to the case of interest, with $c\lesssim 0.75$ (see above), the energy conservation approximately reduces to setting $\theta=$const, and hence Eq. (10) directly yields an evolutional equation for the velocity. This equation is greatly simplified in the case $\theta\lesssim 0.2\pi$:

$$\frac{d}{dt}\frac{c\kappa}{\sqrt{1-c^2}}\approx-\sqrt{1-c^2}\frac{d\kappa}{dx}. \tag{11}$$

A noteworthy consequence of Eq. (11) is that a quiescent soliton ($c=0$) in the apodized grating will start to move with the acceleration $dc/dt\approx -d(\ln\kappa)/dx$.

In order to solve Eq. (11), we notice that the moving soliton actually experiences the smoothly modulated $\kappa(x)$ as a function of time, so that $d\kappa/dt\approx c(d\kappa/dx)$. Substituting this into Eq. (11), the resulting equation can be easily integrated, yielding the final result

$$c^2=1-\frac{\kappa^2}{\kappa_{\rm in}^2}(1-c_{\rm in}^2), \tag{12}$$

where $\kappa_{\rm in}$ and $c_{\rm in}^2$ are the initial values of the reflectivity and velocity. In particular, we notice that, in order to reduce the velocity from the value 0.75 to 0.2, which is a necessary prerequisite for the formation of standing solitons as a result of collision between moving ones (see Introduction), it is enough to use the apodized BG in which the reflectivity is gradually increased by a factor of $\kappa_{\rm fin}/\kappa_{\rm in}\approx 1.48$. If the value of θ is larger ($0.2\pi\lesssim\theta\lesssim 0.5\pi$; still larger values are not relevant as the soliton will be unstable), the analysis of Eq. (10) is slightly more complex, but the final result is quite similar.

IV. COLLISIONS BETWEEN SOLITONS

A. The mode of simulations

In this section, we consider collisions between the BG solitons (2). In a real experiment, an initially launched pulse should pass some distance to shape itself into a soliton. As mentioned above, in previously reported experiments this distance was quite small, ~ 2 cm [10], and hence this is not an important issue. Nevertheless, it may be relevant to separately simulate shaping of an initially launched single-component pulse into a steady-shape BG soliton. This will be done below in Sec. VI.

Simulations of collisions were performed by means of the split-step fast-Fourier-transform method. First, collisions between solitons in the case of repulsion between them, with a phase difference $\Delta\phi_0=\pi$, were considered. It was found that the solitons bounce off each other quasielastically, without generation of any visible radiation or intrinsic vibrations of the solitons, if their initial velocities $\pm c$ are small enough, and the solitons are ''light,'' having a sufficiently small value of θ. Collision-induced radiation becomes conspicuous if the solitons are ''heavier'' or faster; see the example shown in the inset to Fig. 1. Figure 1 displays a boundary in the plane (c,θ) above which the collision results in generation of a noticeable amount of radiation, in the case $\Delta\phi_0=\pi$.

Then, collisions between in-phase solitons, with $\Delta\phi_0=0$ (the case of attraction), were simulated. In this case, a number of various outcomes can be distinguished. A summary of the results is displayed in Fig. 2 in the form of a diagram in the (c,θ) plane, different outcomes being illustrated by the set of generic examples displayed in Fig. 3.

The simplest case is the collision of solitons with small θ (region E in Fig. 2; see also Fig. 4 below). In accordance with the results reported in Ref. [15], these solitons collide elastically, which is easily explained by the fact that they are virtually tantamount to NLS solitons.

B. Merger of solitons and spontaneous symmetry breaking

The most interesting outcome of the collision is *merger* of two solitons into a single one, which takes place in the region $0\leq c<0.2$, $0.15\pi<\theta<0.35\pi$ (area M in Fig. 2). A typical example of the merger is shown in Fig. 3(a), its no-

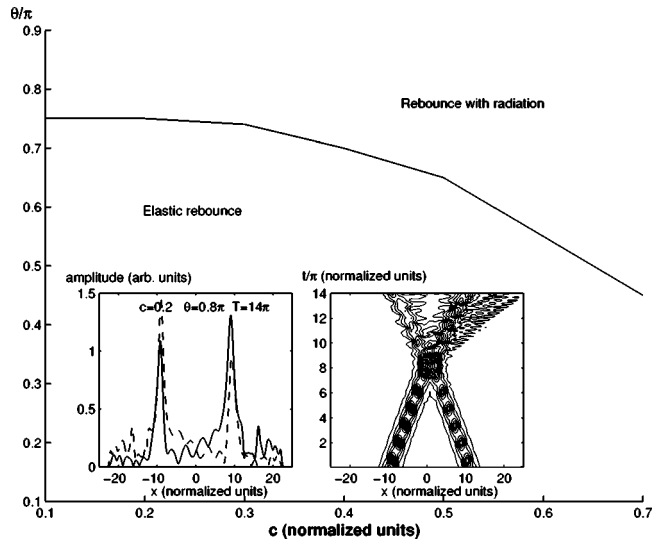

FIG. 1. The border separating regions in the plane $(c,\theta_{\rm in})$ where the collision between π-out-of-phase solitons is elastic or generates significant radiation loss. An example of a collision of the latter type is given in the inset, in which the left and right panels show, respectively, the wave forms $|u(x)|$ and $|v(x)|$ (solid and dashed lines) at the end of the simulation $(t=14\pi)$, and the evolution of the field $|u(x,t)|$ in terms of level contours. Apparent ''oscillations'' of the solitons before the collision in the inset is an artifact due to mismatch between the sampling used for plotting and the numerical grid used for the simulations.

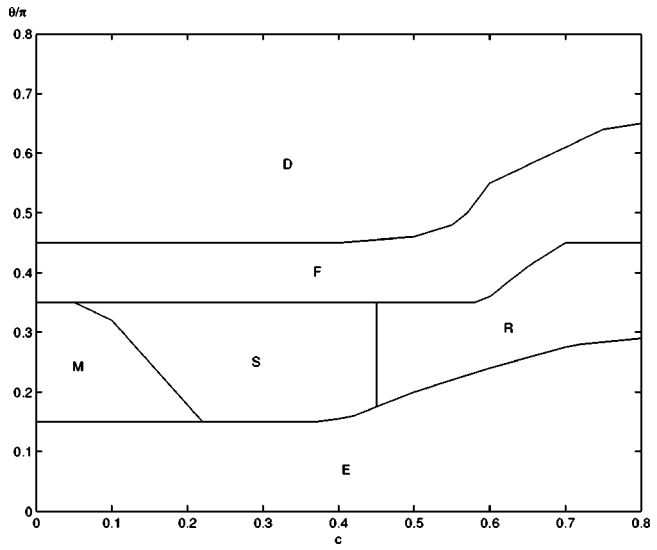

FIG. 2. A diagram in the plane $(c,\theta_{\rm in})$ for different outcomes of the collision between in-phase solitons. In the region *E* the collision is elastic. In the region *M*, the solitons merge into a single pulse. In the region *S*, they separate with velocities smaller than they had before the collision. In the region *R*, the velocities are not affected by the collision, but conspicuous radiation losses are observed. In the region *F*, large radiation loss takes place, and the velocities increase after the collision. In the region *D*, the collision leads to strong deformation of the solitons.

ticeable peculiarities being that the merger takes place after multiple collisions and the finally established soliton demonstrates persistent internal vibrations [see the lowest panel of Fig. 3(a)]. As judged from the lowest panel of Fig. 3(a) (and other similar plots), the amplitudes of these internal vibrations being about 10–20 % of the soliton's amplitudes. In this region of the values of θ (area *M* in Fig. 2), the attraction between initially quiescent $(c=0)$ in-phase solitons, which are placed at some distance from each other, also results in their merger [see Fig. 3(b)]. At the border between the regions *M* and *E*, the interaction between initially quiescent or slow solitons results in their separation after several collisions, which is accompanied by a conspicuous spontaneous symmetry breaking (SSB) [see the example in Fig. 3(c)]. Note that the SSB resembles what was observed in a model of a dual-core fiber grating, in which the nonlinearity and BG were carried by different cores [20]. As in that case, SSB may be plausibly explained by a fact that the ''lump,'' which temporarily forms as a result of the attraction between the solitons in the course of the collision between them, may be subject to modulational instability, and hence a small asymmetry in the numerical noise may provoke conspicuous symmetry breaking in the eventual state. Indeed, it is well known that any spatially uniform solution to Eqs. (1) is modulationally unstable [21], and the instability may extend to a sufficiently broad state, like the above-mentioned ''lump.''

C. Quasielastic collisions

Increase of θ brings one from the region *M* to *F* (Fig. 2), where solitons collide quasielastically, i.e., they separate after the collision, emerging with smaller amplitudes [see Fig. 3(d)]. A noticeable peculiarity of this case is that the collision results in an *increase* of the solitons' velocities, which is seen in the change of the slope of the contour-level plots in Fig. 3(d). We note that, pursuant to Eq. (3), the soliton's energy monotonically increases with c^2; therefore the collision-induced decrease of the amplitude may be explained not only by radiation loss, but also by the increase of the velocities. The acceleration of the solitons due to the collision is more salient if the initial velocity *c* is small; for instance, initially quiescent solitons (with $c=0$) acquire a large velocity after the interaction [see Fig. 3(e)].

As for still heavier solitons, it is known that they are unstable if $\theta>\theta_{\rm cr}\approx 1.011(\pi/2)$ [5,6] (this value pertains to $c=0$; $\theta_{\rm cr}$ very weakly depends on the soliton's velocity [6]). In accordance with this, in the region *D* (Fig. 2) the collision triggers a strong deformation of unstable or weakly stable solitons [see Fig. 3(f)]. At longer times, the strong deformation leads to destruction of the pulses (not shown here explicitly).

If θ is taken in the same range as in the merger region *M*, i.e., $0.15\pi<\theta<0.35\pi$, but with a larger velocity, the collision picture seems ordinary: the solitons separate with some decrease in their velocity and some loss in amplitude. If the initial velocity is still larger, it is possible to distinguish another region, marked *R* in Fig. 2, where the velocity shows no visible change after the collision, but emission of radiation takes place.

Quasielastic collisions can be naturally quantified by the ratio $\theta_{\rm out}/\theta_{\rm in}$ of the soliton's parameter after and before the collision, and by the share of the net initial energy of the

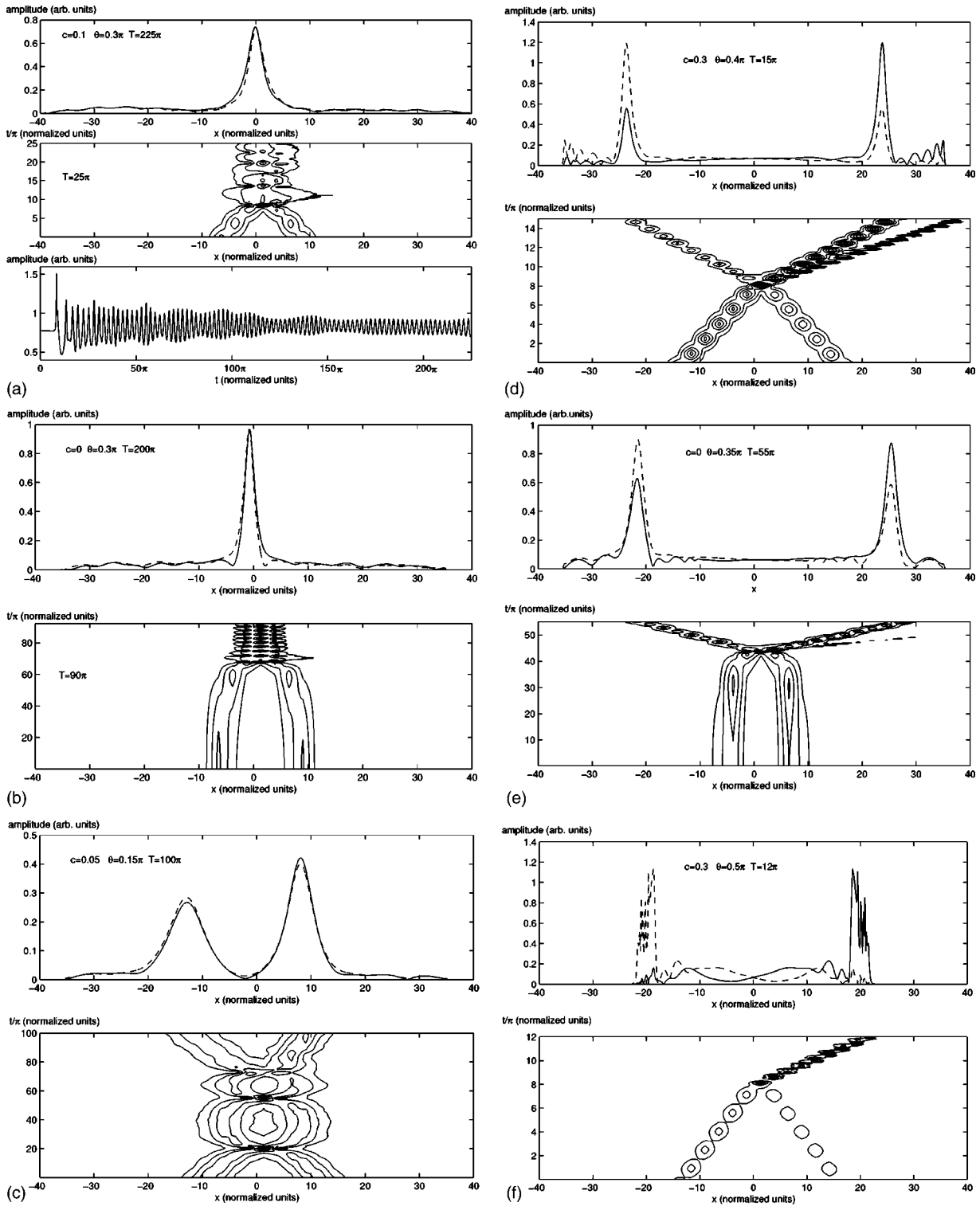

FIG. 3. Typical examples of the collision between in-phase solitons. (a) Merger of the solitons in the region *M* in Fig. 2. They collide several times before the merger, which is accompanied by emission of radiation. The lowest panel exhibits persistent vibrations of the field amplitude $|u(x=0,t)|$. Here and below, the middle and top panels show, respectively, the evolution at a relatively early stage ($t=25\pi$), and the single pulse emerging at $t=225\pi$. (b) Merger of initially quiescent solitons ($c=0$). The lower and upper panels show the evolution at $t<90\pi$ and the emerging single pulse at $t=200\pi$. (c) At the lower edge of region *M* (Fig. 2), solitons undergo multiple collisions before they finally separate. Spontaneous symmetry breaking is evident in the final state. (d) Collision between relatively heavy solitons leads to emission of radiation jets and increase of the velocities (region *F* in Fig. 2). (e) Interaction between two initially quiescent solitons in the region *F* (Fig. 2). (f) Collision between heavy solitons which are weakly stable or unstable (region *D* in Fig. 2) results in strong deformation of the pulses, which is followed by their destruction (not shown here).

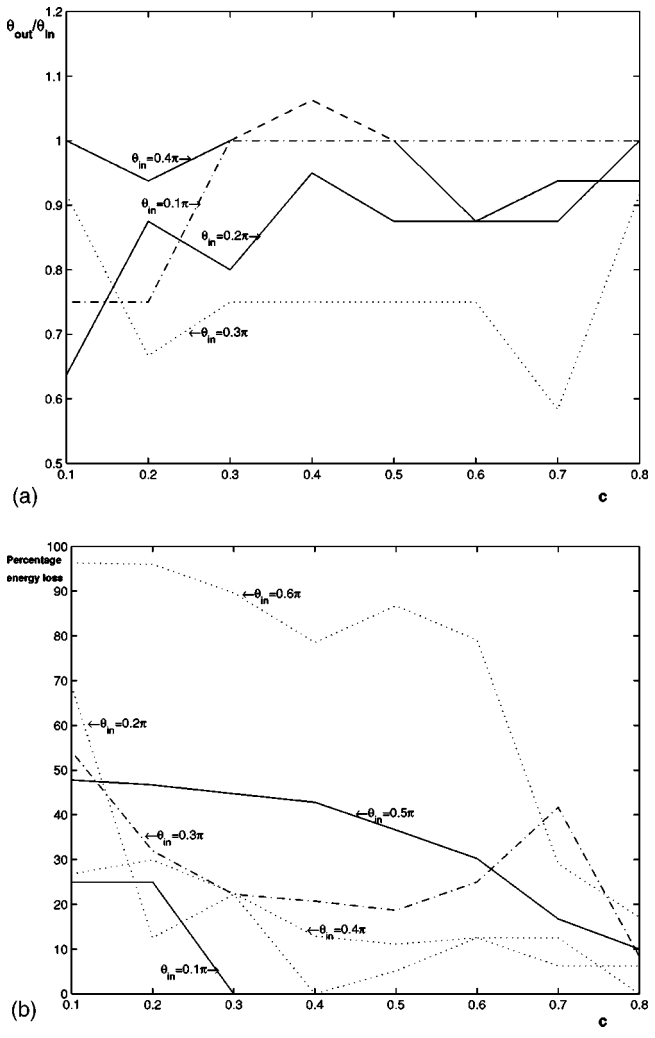

FIG. 4. (a) The ratio of the postcollision soliton's parameter θ_{out}, found from the least-square-error fit of the emerging pulse to the analytical wave forms (2), to the initial value θ_{in}. In this and the next panels, the ratio is shown vs the initial velocity c at different fixed values of θ_{in}. The portion of the line corresponding to $\theta_{\text{in}}=0.4\pi$ with $\theta_{\text{out}}/\theta_{\text{in}}>1$, which formally contradicts energy conservation, is explained by the fact that in this case the actual shape of the emerging pulse is not very close to the analytical one, being more narrow. (b) The relative energy loss due to the collision of two solitons.

solitons which is lost (to radiation) as a result of the collision. To this end, we performed a least-square-error fit of pulses emerging after the collision to the exact soliton solutions (2), aiming to identify the values of θ_{out}, and the postcollision velocity was measured in a straightforward way. The corresponding soliton's energy was then calculated by means of the formula (3).

The results of the computation are shown in Fig. 4. A noteworthy feature, which is obvious in both panels (a) and (b), is that inelastic effects first strengthen with the increase of θ_{in} from very small values (which correspond, as was said above, to the NLS limit) to $\simeq 0.3\pi$, then they weaken, attaining a *minimum*, which corresponds to the most quasielastic collisions, at $\theta_{\text{in}}\approx 0.4\pi$, and then they get stronger again, with increase of θ_{in} up to $\simeq 0.6\pi$. Past the last value, the isolated soliton is strongly unstable by itself and therefore detailed study of collisions becomes irrelevant.

V. MULTIPLE COLLISIONS IN A FIBER RING

Since the main motivation of this work is the possibility of generating a standing pulse by dint of collisions between BG solitons, it is natural to consider multiple collisions that may occur between two solitons traveling in opposite directions in a fiber loop or if a single soliton performs a shuttle motion in a fiber-grating cavity, i.e., a piece of the fiber confined by mirrors (in the latter case, the soliton periodically collides with its own mirror images). An issue for experimental realization of these schemes is to couple a soliton into the loop or cavity. Using a linear coupler to connect the system to an external fiber may be problematic, as repeated passage of the circulating soliton through the same coupler will give rise to conspicuous loss. Another solution may be to add some intrinsic gain to the system, making it similar to fiber-loop soliton lasers, where a soliton-circulation regime may self-start [22]. It is relevant to mention that operation of fiber-ring soliton lasers including BG component(s) as a crucially important element has been reported in much of experimental work [17–19]; in particular, stable circulation of picosecond pulses has been observed.

Still another possibility which lends support to consideration of fiber-grating loops is using a figure-eight lasing configuration [23], in which one loop is made of a BG while the other one provides for the gain. It is relevant to mention that fiber-ring laser schemes even including more than one (up to three) BG-carrying loops were already demonstrated to operate quite efficiently [18]. Further detailed analysis of all these schemes would not be relevant in this paper.

We performed simulations of the multiple collisions between two identical solitons in the loop, imposing periodic boundary conditions. Figure 5(a) shows an example in which the multiple collisions slow down the solitons quite conspicuously, forcing them to merge. As is seen, in this case the solitons undergo two collisions before the merger. The initial values $c=0.3$ and $\theta=0.3\pi$ used in this example show that the multiple collisions in the loop help to increase the maximum initial velocity $c_{\max}$ that admits merger of the two solitons by a factor of 3 (at least) against the single-collision case (cf. Fig. 2). In fact, the largest value of $c_{\max}$ corresponding to the multiple collisions was found to be ≈ 0.4. In other words, a part of the region S from Fig. 2 is absorbed into M in the collision diagram corresponding to the loop configuration. The evolution of the field at the central point $|u(x=0)|$, which is also displayed in Fig. 5(a), demonstrates that the emerging zero-velocity pulse is again a breather [cf. Fig. 3(a)].

Another example of multiple collisions in the loop is shown in Fig. 5(b), where the solitons initially have $\theta=0.3\pi$ and $c=0.7$, belonging to the region R of Fig. 2. In this case, the solitons hardly undergo any slowing down due to the collisions, while they keep losing energy. Due to the gradual decrease of θ, which is related to the energy by Eq.

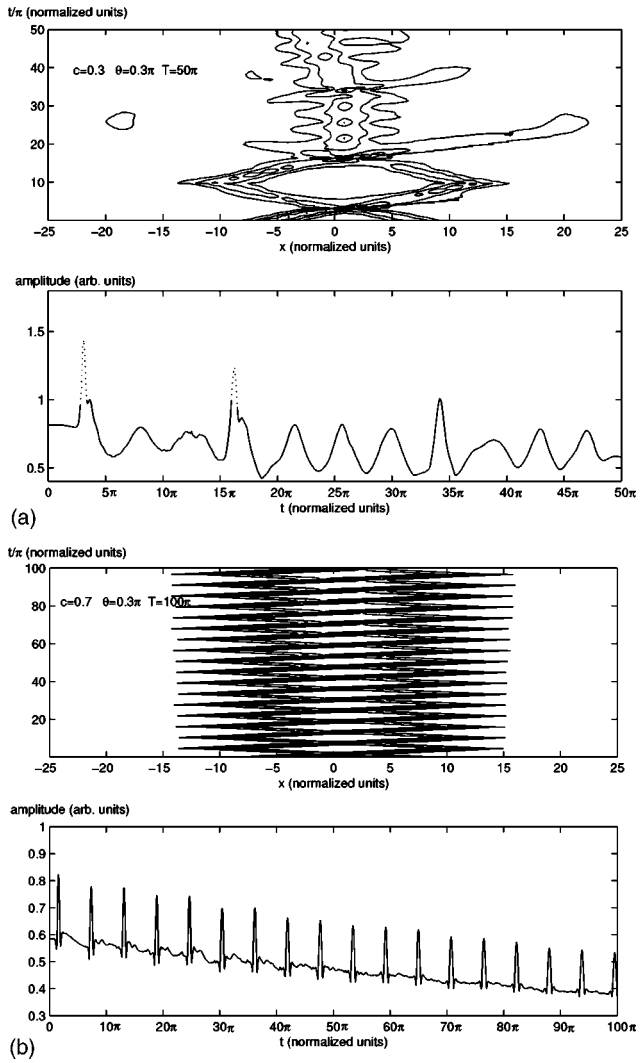

FIG. 5. (a) Multiple collisions between two solitons with the initial value $\theta=0.3\pi$ and initial velocity ± 0.3 in the loop configuration. The upper and lower panels, respectively, show the global evolution of the field $|u(x,t)|$ and the evolution of its maximum. In the lower panel, the dotted parts of the curve mark two collisions (maximum overlappings) between the two solitons before they merge into a single pulse. (b) Multiple collisions between solitons with the initial value $\theta=0.3\pi$ and initial velocities ± 0.7 in the loop configuration.

(3), the solitons gradually drift to the region E (see Fig. 2), where the collision becomes elastic.

VI. EFFECT OF A LOCALIZED DEFECT ON THE COLLISION

In Refs. [11] and [12], it has been found that local attractive defects can trap gap solitons. This fact suggests the possibility that the merger of two colliding solitons might be assisted by a defect placed at the collision point. We investigated the effect of two kinds of local defects, which represent BG suppression or increase of the refractive index, corresponding, respectively, to $\kappa>0$ and $\Gamma>0$ in Eqs. (6) (the single collision was considered in this case).

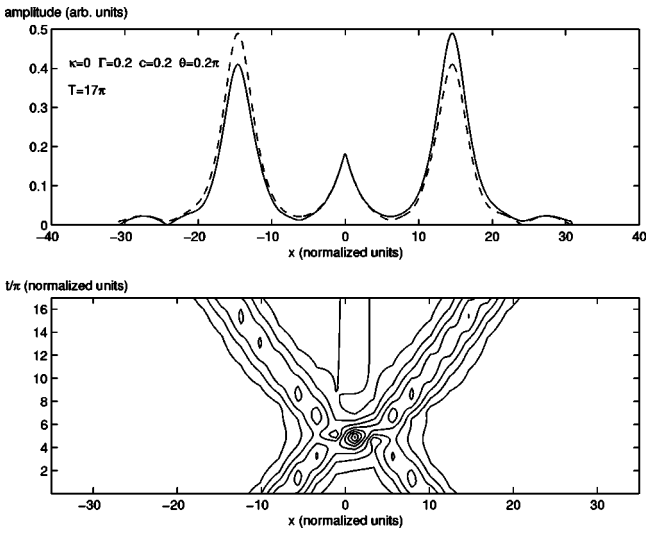

FIG. 6. The collision between solitons with $\theta=0.2\pi$ and velocities $c=\pm 0.2$ in the case when a local perturbation of the refractive index, with $\Gamma=0.2$ [see Eqs. (6)], is placed at the collision point. The defect traps a small-amplitude soliton.

We have found that attractive defects of either type do not actually catalyze formation of a pinned pulse that would retain a large part of the energy of the colliding solitons. Nevertheless, a relatively small part of the energy gets trapped by the defect, and a small-amplitude pinned soliton appears (see the example in Fig. 6), which is displayed for the case of a local refractive-index perturbation, i.e., $\Gamma>0$, $\kappa=0$. Local BG suppression, accounted for by $\kappa>0$, produces a similar effect. We have also checked that repulsive local defects (negative Γ or κ) do not produce any noticeable effect either.

VII. SPECIAL EFFECTS IN THE SINGLE-SOLITON DYNAMICS

A. Transformation of an input pulse into a Bragg-grating soliton

As mentioned above, signals that are coupled into a fiber grating in a real experiment are not ''prefabricated'' BG solitons, but rather pulses of a different form, which should shape themselves into solitons. After that, one can consider collisions between them, as was done above. For this reason, it makes sense to specially consider self-trapping of BG solitons from an input pulse in the form of a NLS soliton,

$$u_0(x)=\eta\,\mathrm{sech}(\eta x)\exp(-ikx),\quad v_0(x)=0, \tag{13}$$

where η and k are constants, or a Gaussian pulse,

$$u_0(x)=A\exp(-\gamma x^2),\quad v_0(x)=0. \tag{14}$$

The energy of the NLS soliton (13), defined as per Eq. (3), is 2η, and the energy of the pulse (14) is $A^2\sqrt{\pi/\gamma}$.

In fact, we also simulated the transformation of input pulses of other shapes, with the conclusion that the results are quite similar to those briefly presented below for the sech and, especially, Gaussian inputs. In this connection, it is relevant to mention that, before feeding the input pulse into the

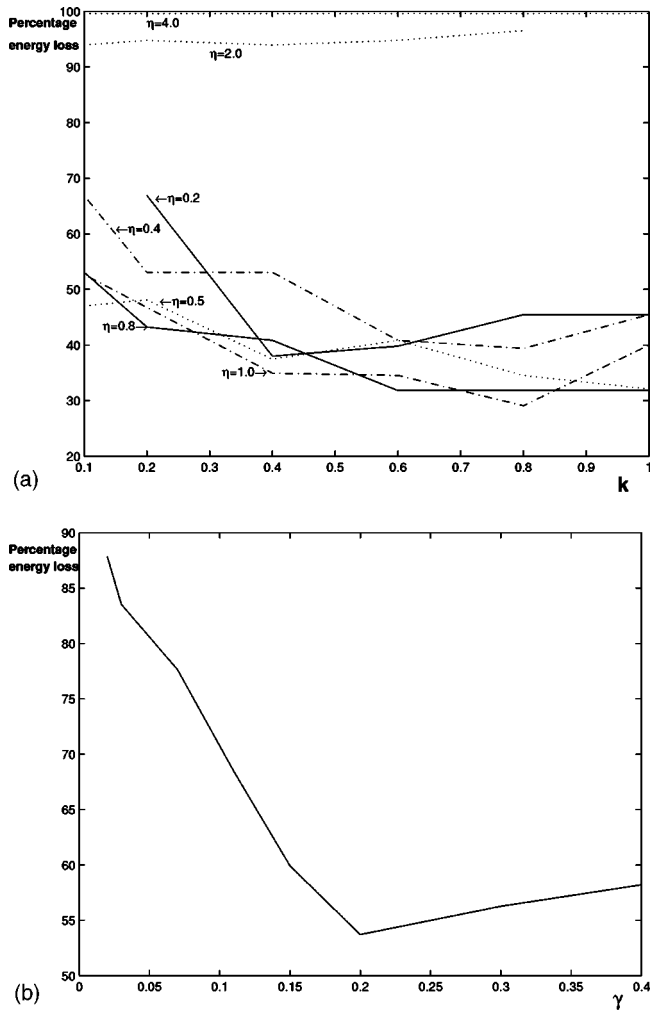

FIG. 7. (a) The relative energy loss in the process of self-trapping of the Bragg-grating soliton from the initial NLS-soliton pulse (13) vs the soliton speed parameter k in Eq. (13) (at fixed values of the amplitude η). (b) The same energy loss, for the case of the initial Gaussian pulse (14) with $A=1$ and $\kappa=1$, vs the inverse square width γ.

fiber grating, it can pass through an ordinary nonlinear fiber, which will help to preliminarily reshape any pulse into a NLS soliton of the form (13).

Transformation of the pulses into a BG soliton was simulated directly within the framework of Eqs. (1). For the NLS soliton, the results are summarized in Fig. 7(a), in the form of plots showing the share of the initial energy lost into radiation [cf. Fig. 4(b)]. A noteworthy feature revealed by the systematic simulations is that, with the increase of the parameter η that measures the amplitude and inverse width of the initial pulse (13), the energy-loss share first decreases, attaining an absolute minimum at $\eta \simeq 0.8$–1.0, and then quickly increases. The fact that the relative energy loss becomes very large for large η is easy to understand, as the initial energy of the pulse (13) increases indefinitely with η, while the energy of an emerging stable BG pulse, with $\theta \leqslant 1.011(\pi/2)$ and $c^2<1$, cannot exceed (in the present notation) $E_{\max}=(4/3)\pi$ [see Eq. (3)]. Thus, an optimal shape of the sech input signal, which provides for the most efficient generation of the BG soliton, is suggested by these results.

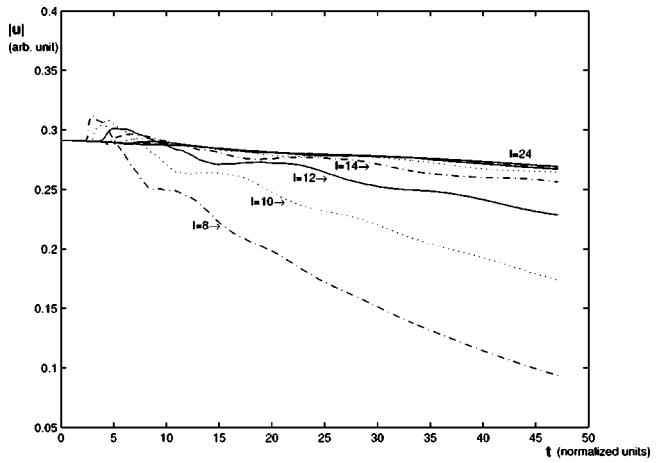

FIG. 8. Decay of the field $|u(x,t)|$ at the central point of the finite fiber grating of length l due to the energy loss through the free ends.

For the initial Gaussian pulse (14), similar results are shown in Fig. 7(b), for the case $A=1$. It can be seen that an optimal value of the width factor γ, for which the largest share of the initial energy is retained in the resulting gap soliton, can be found in this case too, being ≈ 0.2. A single pulse is formed around this value, while much smaller or larger values of γ (such as $\gamma \lesssim 0.02$ or $\gamma \gtrsim 1$) give rise to multiple BG solitons (similarly, in the case of the NLS soliton initial pulse considered above, formation of multiple BG solitons is also observed when the energy of the initial input pulse is much larger than that of the resulting BG soliton). With the increase of the amplitude A of the initial Gaussian pulse (14), the energy share that is retained in a single BG soliton decreases, similar to what was observed in Fig. 7(a) with the increase of the amplitude η of the NLS soliton (13).

B. Decay of the soliton in a finite-length fiber grating with free ends

In an experiment (unless the fiber loop or cavity is used), a standing soliton will be created in a fiber grating with open edges. Then some energy leakage will take place through the free ends of the fiber segments. From the exact solution (2) it follows that the leakage is exponentially small if the segment's length l is much larger than the soliton's spatial width, which is ~ 1 mm in a typical situation [10,14]. Moreover, the energy leakage through the loose ends can be easily compensated (along with intrinsic fiber loss) by local gain [14]. Nevertheless, it is an issue of interest to find the soliton's decay rate due to the leakage.

We addressed this issue, simulating Eqs. (1) with the free boundary conditions $u_x=v_x=0$ set at the edges of the integration domain. In Fig. 8, we show the decay of the soliton's amplitude in time, for different values of the domain's length, with the initial value $\theta_{\text{in}}=0.51$. The initial increase of the amplitude is a result of temporary self-compression of the pulse due to its interaction with the edges. As a reference, we mention that, in the case of the shortest fiber grating

considered here, with $l=8$, it takes a time $t=42.2$ for a decrease of the amplitude by a factor of e.

VIII. CONCLUSION

We have presented the results of systematic studies of collisions between moving solitons in fiber gratings. Various outcomes of the collision were identified, the most interesting one being merger of the solitons into a single zero-velocity pulse, which suggests a way to create pulses of ''standing light.'' The merger occurs for solitons whose energy takes values between 0.15 and 0.35 of its maximum value, while the velocity is limited by $c_{\max}\approx 0.2$ of the limit velocity. If the energy is larger, another noteworthy outcome is acceleration of the solitons as a result of the collision, especially when their initial velocities are small. In the case when the solitons pass through each other, the inelasticity of the collision was quantified by the relative energy loss. If the energy exceeds the soliton's instability threshold, the collision results in strong deformation of the solitons, which is followed by their destruction. Simulations of multiple collisions between two solitons in the fiber-loop configuration show that the largest initial velocity admitting the merger increases to $c\leqslant c_{\max}\approx 0.4$ of the limit velocity. It was also shown that attractive local defects do not alter the overall picture, although a small-amplitude trapped pulse appears in this case. It was also shown in an analytical form that fast BG solitons can be efficiently slowed down (to values of the velocity that admit the fusion of colliding solitons) by passing them through an apodized fiber grating with a gradually increasing value of the Bragg reflectivity. Additionally, specific effects were investigated in one-soliton dynamics, such as transformation of a single-component input pulse into a Bragg-grating soliton, and decay of the soliton in a finite-length fiber grating due to the energy leakage through loose edges.

ACKNOWLEDGMENTS

One of the authors (B.A.M.) appreciates the hospitality of the Optoelectronic Research Center at the Department of Electronic Engineering, City University of Hong Kong.

[1] R. Kashyap, *Fiber Bragg Gratings* (Academic Press, San Diego, 1999).
[2] C.M. de Sterke and J.E. Sipe, Prog. Opt. **33**, 203 (1994).
[3] A.B. Aceves and S. Wabnitz, Phys. Lett. A **141**, 37 (1989).
[4] D.N. Christodoulides and R.I. Joseph, Phys. Rev. Lett. **62**, 1746 (1989).
[5] B.A. Malomed and R.S. Tasgal, Phys. Rev. E **49**, 5787 (1994).
[6] I.V. Barashenkov, D.E. Pelinovsky, and E.V. Zemlyanaya, Phys. Rev. Lett. **80**, 5117 (1998); A. De Rossi, C. Conti, and S. Trillo, *ibid.* **81**, 85 (1998).
[7] A.V. Yulin, D.V. Skryabin, and W.J. Firth, Phys. Rev. E **66**, 046603 (2002).
[8] J. Marangos, Nature (London) **397**, 559 (1999); K.T. McDonald, Am. J. Phys. **68**, 293 (2000).
[9] J.E. Heebner, R.W. Boyd, and Q.H. Park, Phys. Rev. E **65**, 036619 (2002).
[10] B.J. Eggleton, R.E. Slusher, C.M. de Sterke, P.A. Krug, and J.E. Sipe, Phys. Rev. Lett. **76**, 1627 (1996); C.M. de Sterke, B.J. Eggleton, and P.A. Krug, J. Lightwave Technol. **15**, 1494 (1997).
[11] R.H. Goodman, R.E. Slusher, and M.I. Weinstein, J. Opt. Soc. Am. B **19**, 1635 (2002).
[12] W.C.K. Mak, B.A. Malomed, and P.L. Chu, J. Opt. Soc. Am. B **20**, 725 (2003).
[13] C.M. de Sterke, E.N. Tsoy, and J.E. Sipe, Opt. Lett. **27**, 485 (2002).
[14] W.C.K. Mak, B.A. Malomed, and P.L. Chu, Phys. Rev. E **67**, 026608 (2003).
[15] N.M. Litchinitser, B.J. Eggleton, C.M. de Sterke, A.B. Aceves, and G.P. Agrawal, J. Opt. Soc. Am. B **16**, 18 (1999).
[16] Yu.S. Kivshar and B.A. Malomed, Rev. Mod. Phys. **61**, 763 (1989).
[17] J.J. Pan and Y. Shi, Electron. Lett. **31**, 1164 (1995); M.J. Guy, J.R. Taylor, and R. Kashyap, *ibid.* **31**, 1924 (1995); P.K. Cheo, L. Wang, and M. Ding, IEEE Photonics Technol. Lett. **8**, 66 (1996); H. Inaba, Y. Akimoto, K. Tamura, E. Yoshida, T. Komukai, and M. Nakazawa, Electron. Commun. Jpn., Part 2: Electron. **85**, 21 (1999); X.W. Shu, S. Jiang, and D.X. Huang, IEEE Photonics Technol. Lett. **12**, 980 (2000); L. Talaverano, S. Abad, S. Jarabo, and M. Lopez-Amo, J. Lightwave Technol. **19**, 553 (2001); Y. Wang, S.C. Tjin, J. Yao, J.P. Yao, L.M. He, and K.A. Ngou, Opt. Commun. **211**, 147 (2002); J.N. Maran, S. LaRochelle, and P. Benard, *ibid.* **218**, 81 (2003).
[18] C.C. Lee, Y.K. Chen, and S.K. Liaw, Opt. Lett. **23**, 358 (1998).
[19] J. Yao, J.P. Yao, Y. Wang, S.C. Tjin, Y. Zhou, Y.L. Lam, J. Liu, and C. Lu, Opt. Commun. **191**, 341 (2001).
[20] J. Atai and B.A. Malomed, Phys. Rev. E **64**, 066617 (2001).
[21] A.B. Aceves, C. De Angelis, and S. Wabnitz, Opt. Lett. **17**, 1566 (1992).
[22] L.E. Nelson, D.J. Jones, K. Tamura, H.A. Haus, and E.P. Ippen, Appl. Phys. B: Lasers Opt. **65**, 277 (1997).
[23] T.O. Tsun, M.K. Islam, and P.L. Chu, Opt. Commun. **141**, 65 (1997).